Thermal relaxation and critical instability of near-critical fluid microchannel flow

Lin Chen,[1] Xin-Rong Zhang,[1,*] Junnosuke Okajima,[2] and Shigenao Maruyama[2]
[1]*Department of Energy and Resources Engineering, College of Engineering, Peking University, Beijing 100871, China*
[2]*Institute of Fluid Science, Tohoku University, Katahira 2-1-1, Aoba-ku, Sendai 980-8577, Japan*
(Received 23 February 2012; revised manuscript received 31 December 2012; published 30 April 2013)

We present two-dimensional numerical investigations of the temperature and velocity evolution of a pure near-critical fluid confined in microchannels. The fluid is subjected to two sides heating after it reached isothermal steady state. We focus on the abnormal behaviors of the near-critical fluid in response to the sudden imposed heat flux. New thermal-mechanical effects dominated by fluid instability originating from the boundary and local equilibrium process are reported. Near the microchannel boundaries, the instability grows very quickly and an unexpected vortex formation mode is identified when near-critical thermal-mechanical effect is interacting with the microchannel shear flow. The mechanism of the new kind of Kelvin-Helmholtz instability induced by boundary expansion and density stratification processes is also discussed in detail. This mechanism may bring about innovations in the field of microengineering.

DOI: 10.1103/PhysRevE.87.043016 PACS number(s): 47.61.−k, 45.80.+r, 47.32.C−, 47.55.pb

I. INTRODUCTION

As the gas-liquid critical point is approached in supercritical fluids, strong anomalies can be found in thermal and transport coefficients [1]. The isothermal compressibility and thermal expansion both grow dramatically while the thermal diffusivity tends to zero. These specific properties induce special coupling processes of thermal equilibrium and mechanical disturbance or instability. In closed systems, an additional adiabatic heat transfer mechanism called the piston effect (PE) has been identified independently by several teams [2]. When heating the boundary of near-critical fluid, a very expandable, thin, diffusive layer is formed, which compresses the bulk fluid and causes the temperature of the bulk fluid to increase at acoustic time scale. Therefore heat is transported much faster than simple diffusion in such systems by the thermal-mechanical expansion and compression process, like a thermal piston [3–5]. Such thermal-mechanical process occurs in near-critical fluids and special focus has consequently been laid on experimental justifications and application development [6]. The possibility of long-distance heat transport in weightlessness has also been experimentally investigated recently [7]. Later, the effect of boundary condition on the expanding acoustic thermal equilibrium process was discussed and the critical cooling effect was suggested responsible for abnormal temperature behaviors under various boundary conditions [4]. Indeed, as one kind of near-critical thermal-mechanical process, this specific behavior contributes to normal heat convection or relaxation both in closed systems or open systems; for example, the thermal oscillations of near-critical ^{3}He at Rayleigh-Bernard threshold when heating the fluid from the bottom wall of a shallow cavity [8,9].

Recent studies into the basic behaviors of near-critical pure fluid have extended to two-sided boundary heat flux input [10], and the respective time scale analysis will cover from acoustic time scale, intermediate, to diffusion time scales [4]. Also, it is suggested that strong boundary thermal-mechanical effect was first found in a closed system under microgravity and the strong compression and reflection only happen in constrained flow (where it is called the piston effect; under global or local heating) [11]. Therefore, recently the interest in open systems and the behaviors under coupled effects of the near-critical thermal-mechanical process and gravity have also been suggested. The first studies were of small size channel thermal effects in cylindrical cells (with fluid thickness $L = 10$ mm) [5] or thermal plumes [12]. Instead of "critical slowing down" (due to small thermal diffusivity in the boundary thermal relaxation process), the expanding thermal boundary greatly affects the convection process and flow structure [13]. The local equilibrium process and transient temperature and velocity behave differently during those processes.

This paper is devoted to the general response of a developed isothermal near-critical fluid flow when subjected to boundary heating. We present interesting findings on the near-critical hot boundary layer (HBL) expansion and its interactions with bulk flow. New boundary instability behaviors are presented with ensuing vortex formation and micromixing processes in microchannels. The origin of the current transient unstable thermal relaxation is found to be near-critical boundary thermal-mechanical effects, which is similar to the evolution of PE boundaries in closed systems. Respective time scales and transient stability evolution are also analyzed. Current results are identified with a new type of Kelvin-Helmholtz instability where the expanding boundary serves as the perturbation source and suppresses the effect of gravity in microchannels. This may open new possibilities in microengineering and supercritical processes.

II. MODEL

For the sake of simplicity, we consider a two-dimensional microchannel with length ($L = 0.05$ m) and height ($D = 0.1$ mm). In this simulation, the channel, with a typical large length and height ratio of 500, has near-critical fluid confined between two rigid planes. As near-critical fluid is very expandable even under very small heat input, the local thermal relaxation process can be very different from normal fluids in microchannels. Previously it was generally expected

*Corresponding author: zhxrduph@yahoo.com

that normal fluids would be stable under similar conditions. However, thermal vibrations have been found in near-critical fluids in a one-dimensional (1D) configuration [14], and the local perturbation from the HBL and respective "thermal jets" caused by boundary thermal-mechanical expansion become the main reason for rapid heat equilibrium in near-critical fluids, compared to the case of perfect gas [3]. The first step of simulation was to conduct an isothermal wall and developed near-critical flow in the microchannel. The two side channel walls are first kept isothermal until the near-critical microchannel flow converges, and then the fluid is subjected to two-sided heat flux Q until thermal equilibrium is reached. The equations of motion are the Navier-Stokes equations, which are solved together with the energy equation and the equation of state as follows:

$$\frac{\partial(\rho C_p T)}{\partial t} + \nabla\cdot(\rho \mathbf{V} C_p T) = \nabla(\lambda \nabla T) + T\beta_P \frac{\partial P}{\partial t} + \Phi \quad \text{energy;}$$

$$\rho = \rho_0 + \rho_c \chi_T (P - P_0) - \rho_c \beta_P (T - T_0) \quad \text{state,}$$

where β_P is the isobaric thermal expansion coefficient, χ_T is the isothermal compressibility (both are nonlinear parameters, as the properties diverge near the critical point. λ is the thermal conductivity, C_P is the specific heat, $\Phi = \sigma_{ij}(\partial u_i/\partial x_i)$ is the dissipation function with σ_{ij} the viscous stress tensor and u_i the velocity components, and P_0 and T_0 are initial pressure and temperature. The thermal-transport coefficients are obtained from the NIST standard database [15]. The current model has been tested and validated in previous studies [9] treating near-critical thermal oscillation and equilibrium processes. Indeed, special difficulties occurred when considering the coupled convection and thermal propagation process in near-critical fluids. In previous studies of near-critical heat and mass transfer, divergences in correlation length, time and fluid properties were found, especially at hot boundaries where steep gradients in fluid parameters are seen [1,3–5]. Nonuniform grids were carefully generated in the calculation domain (with around 3×10^5 mesh grids for the $D = 100\ \mu$m case) and refined specfically for the boundary and internal areas during the initial studies to ensure that mesh independent results are obtained. Still the comparison between the mesh size and the small scale divergences (or fluctuations) of near-critical fluid would be useful for the study of such near-critical phenomena. The ratio of mesh size to correlation length ($\sim |\varepsilon_T|^{\nu}$) across the current near-critical boundary layers ranges from 0.2 to 1.0, and in the bulk the effect is generalized as the critical fluctuations will decay with the increase of "distance" from the critical point during heating. The respective correlation time for this divergence is also much smaller (<0.01%) than that of the current pressure relaxation or thermal-mechanical relaxation time scales. For the current model, a finite volume method was used and the method of solution has been validated [9].

The focus of the current study is the thermal disturbance and convection onset equilibrium process in microchannel flows of near-critical fluids. Steady state theories for the onset of convection exist for incompressible and moderately compressible fluids; however, interesting phenomena occur when the fluid approaches the near-critical region [3,9]. Currently, we choose CO_2 with inlet $T_{\text{in}} = T_0 = (1 + \varepsilon_T)\, T_c$ and $P_{\text{in}} = P_0 = (1 + \varepsilon_P)\, P_c$, where T_c and P_c are, respectively, the critical temperature and pressure. When the microchannel scaling effect is considered, supercritical fluid shows no surface tension, which brings further simplicity for simulation.

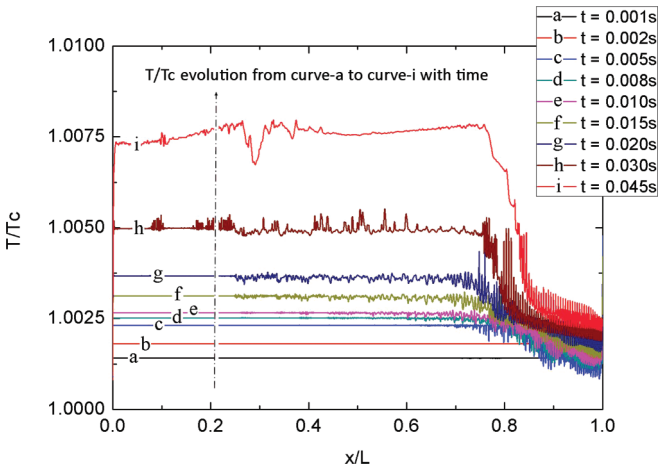

FIG. 1. (Color online) Evolution of wall temperature propagation with inlet Re = 13.40 and $Q = 10\,000$ W/m^2; thermal equilibrium speeding-up is found for near-critical CO_2 ($\varepsilon_T = 0.000\,23$ and $\varepsilon_P = 0.016\,26$); the growth of perturbation and temperature collapse indicate critical convection onset instability.

III. RESULTS

Using the above model, we performed simulations with $\varepsilon_T = 0.000\,23$ and $\varepsilon_P = 0.016\,26$, with the critical values of CO_2 fluid as $T_c = 304.13$ K, $P_c = 7.38$ MPa, and $\rho_c = 467.6$ kg/m^3. Thus the inlet fluid flow parameters (T,P,ρ) are slightly above the critical point. Two-sided heat flux $Q = 10\,000$ W/m^2 was applied after the microchannel flow reached isothermal steady state. The transient evolution of wall temperature is plotted in Fig. 1 (for inlet Re = 13.40). In the current microchannel model, gravity is neglected as the calculated Froude number is much smaller than unity, therefore it is possible to ignore the effect of gravity. Indeed the upper wall (Fig. 1) temperature evolution is almost the same as the lower wall (not shown here). It is seen from Fig. 1 that after heat flux was applied, and thermal convection commences, the temperature collapses are found even in as small time scales as 10^{-3} s. It is shown that $(T - T_c)$ drops by 50% after the heat flux is applied for about 10^{-2} s. Also the temperature drops and collapse grow from the channel outlet side through the flow, while the main wall temperature increases with time. Such collapse indicates much faster thermal equilibrium process in the microchannel than steady thermal convective (or steady thermal diffusion) channel flow condition in normal fluid.

Comparisons of microchannel velocity and density fields with time and position are presented in Fig. 2. As shown, very thin boundary layers are formed after heat is applied at two walls, where the fluid density soon drops about 8% below the main flow [see Fig. 2 ($t = 2$ ms)]. Consequently the thin hot boundary evolves to show local hot spots. Indeed local pressure gradients are found in both horizontal and vertical directions, forming a local intrusion (with higher temperature, "hot spot")

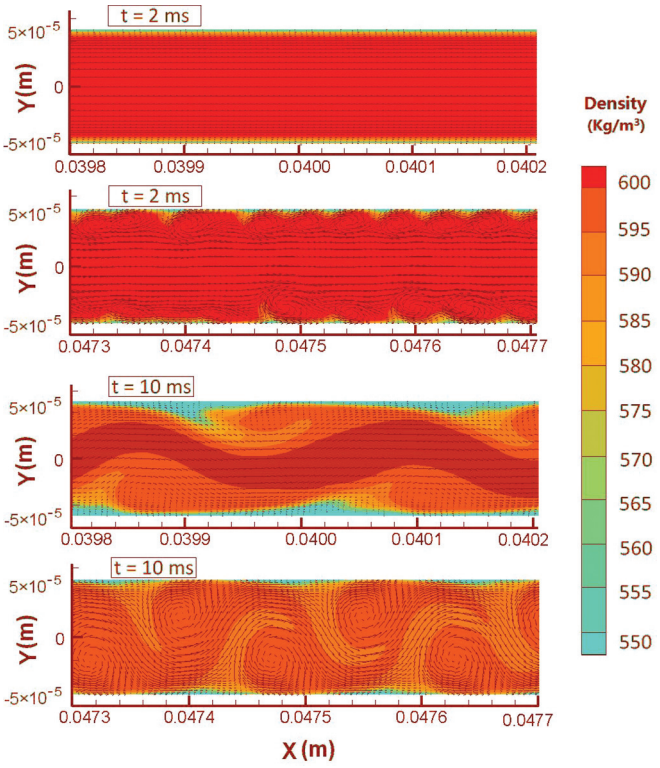

FIG. 2. (Color online) Flow stream field and density evolution with time and position (at 2 and 10 ms, respectively; position around $x/L = 0.80$ and 0.95; $Q = 10\,000$ W/m^2; inlet Re = 13.40). The boundary perturbation by hot spot interacting with main flow is captured. Vortex evolves from two hot boundaries and soon expands to the two side walls as shown by the velocity vectors in the above figure. The density is contoured by color bars and the velocity is presented in vector form (by arrows).

from the boundary layer into the main flow [see Fig. 2 (t = 2 ms), where the flow streams are shown in vector form]. It is seen from Fig. 2 that the instability grows both with time and position. The instability produces vortices across the channel near the microchannel end part [see Fig. 2 (t = 10 ms)]. The vortex size is estimated to be similar to the channel height (0.1 mm in Fig. 2). Such hot spot formation and disturbance has also been reported [16] for the steady near-critical diffusion process in a Rayleigh-Bernard configuration (from initial static state) under gravity. The current model starts from a developed isothermal state with microchannel configuration suppressing the effect of gravity. The symmetric development of unstable hot spots and vortices has not been reported in the literature and it represents a fundamentally new mechanism of unstable relaxation induced by near-critical fluid thermal-mechanical effect.

As has been discussed, the above process happens at very small time scales. The vortex will expand toward the microchannel walls causing strong fluid mixing and helping to establish thermal equilibrium. In the current study, the vortex finally diffuses, thermal equilibrium is reached, and the microchannel flow becomes laminar with static thermal and viscous boundaries. As discussed, the current model is a two-dimensional (2D) open system where traditional PE will not take place as no closed reflective boundary exists [11]. However, the near-critical thermal-mechanical effect (with PE boundaries, as one case for a closed system) can still play a special role in the development of thermal boundaries. With immersed heat source models [17], rapidly expanding thin hot boundary layers form the disturbance hot spots, which greatly affect the convection structure. Such thermal disturbance and compression from the expanding boundary creates acoustic waves (thermal-acoustic or mechanical effect) in closed systems [2] and in the current open flow system it expands directly into the main fluid, thus forming unstable flow at low Reynolds number condition.

Indeed, if the current system reaches thermal equilibrium by pure thermal diffusion, the characteristic time scale will be $t_d = D^2/D_T = 1.15$ s, where D_T is the thermal diffusivity of near-critical CO_2 (using initial values). The current transient process happens within 0.4 s and vortex formation time scale is calculated similar to that of piston effect time scale with the same thermal-mechanical origins as first predicted by Onuki *et al.* [2] as $t_{\rm PE} = t_d/(\gamma - 1)^2 = 8$ ms, where γ is the specific heat ratio. Traditional studies on piston effect have begun very near to the critical condition with very small perturbation on the boundary, which allows very small changes of properties in the bulk fluid [18]. The thermal-mechanical expansion-compression process is dependent on how close the fluid state is to the critical point. For open systems, such initial conditions should be equally important [7,13]. With the development of the system through the critical point, properties behave divergently as discussed. From the ratio of the thermal-mechanical time (piston effect time for closed system) scale $t_{\rm PE}$ to the thermal diffusion time scale t_d, it is hard to track and estimate these divergences, especially during the nonlinear changes in thermal diffusivity and viscosity [17]. Therefore in the evolution of instability and formation of the vortex, the acoustic waves are not stable as in closed PE systems [2]. In a discussion of thermal-acoustic waves near the critical point, Carles [17] also reported the instability of density-pressure evolution in the initial heat input period (with several initial density stages measured).

The pressure distribution and perturbation velocity (y velocity) across the channel are plotted perpendicular to the stream flow direction at position $x/L = 0.98$ in Figs. 3(a) and 3(b). It is seen that the pressure and perturbation velocity (in the y direction) both fluctuate with time. Though the fluctuations are not periodic due to the characteristic time scale changes discussed above, the evolution of the acoustic expanding process is seen. For example, in Fig. 3(a) the pressure increases at time 2.5×10^{-4} s and drops at 4.5×10^{-4} s and then fluctuates again under constant influx heating. Figure 3(b) also shows the symmetric two-sided expanding process with peak perturbation velocity near the diffusion thermal boundary contacting with the main flow. Similar oscillations have also been found in Refs. [14,17] when near-critical fluid confined between heating rigid planes is considered (with relative larger channel size, such that the perturbation velocity is three to four times larger than in the current study; such kind of vibration or perturbation is easily seen in confined near-critical fluids). Also, the velocity differences across the boundary contact line with the bulk contribute to the unstable evolution. Though supercritical fluids can be of low viscosity, the scaling across

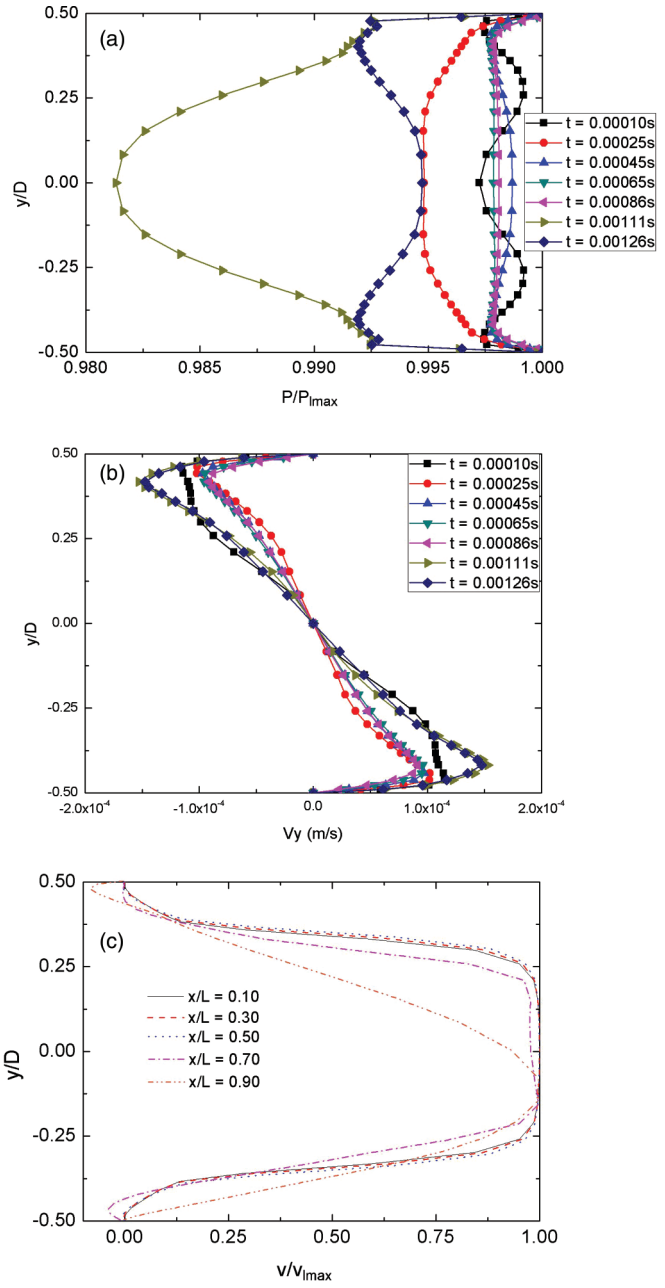

FIG. 3. (Color online) Boundary thermal-acoustic effects and their evolution. (a) Evolution of pressure field; (b) two-side perturbation velocity (perpendicular to stream flow at small time scale); (c) horizontal flow velocity profiles. For (a) and (b) position $x/L = 0.98$ is chosen as representative, where the x axis is the midline of the horizontal channel direction. P/P_{lmax} is pressure normalized by local maximum values. v/v_{lmax} is velocity normalized by local maximum values. The parameters are the same as Fig. 2(c) and show several representative cross faces along the x direction. The velocity shear near the boundary layer shows the typical supercritical fluid characteristic, with very thin and relative steep gradients, which contributes to the KH instability; reversed vortex flow can be found for the $x/L = 0.7$ or 0.9 parts; more instabilities are found for the downward flow in the microchannel, which indicates the KH instability growth with position.

the critical point still shows discrepancies with normal fluids, especially under a different Re number condition between the boundary low velocity flow and the relative high Re bulk flow. The fluctuation in perturbation velocity induces the main flow instability growth with time and locally forms the vortex from the boundaries.

Vortex formation is of engineering interest as part of the rapid development in supercritical technology and Micro-Electro-Mechanical Systems (MEMS) related fields. Transient sudden mixing or heat flux induced instability can also be applied both in gravity and microgravity conditions in microchannel flow. However, theoretical explanations of the instability (where gravity is not important in microchannels) can also be important. Indeed, the current microchannel instability can be categorized to be a type of Kelvin-Helmholtz (KH) instability as with the characteristic of largely stratified layers of fluid by thermally induced density heterogeneity. The classical KH instability, due to density stratification and/or velocity shear was first introduced by Lord Kelvin (1871) [19], where gravity is the typical source of instability. In the current model, the gravity wave, as the instability source, is replaced by pressure gradient across the two heating planes, where perturbation waves perpendicular to the stream flow are formed and strong stratification of density and velocity are also generated in near-critical CO_2 fluid though the channel is of microscale. The current instability in microchannel thermal relaxation is still within the KH instability range, but its perturbation source comes from HBL thermal-mechanical expansion, which is a new kind of instability origin which suppresses gravity effect.

From classical KH instability models, any small stratification will lead to fluid "tear off" however small the perturbation is (with perturbation source provided). By analogy to the traditional analysis when KH instability was induced under gravity [19], a modified Richardson number was defined according to the thermal-dynamic conditions (especially suppression of gravity and added the dominant factor of density and velocity stratifications):

$$R_i = \frac{1}{\rho^2}\frac{(dp/dy)(d\rho/dy)}{(du/dy)^2},$$

where the pressure gradient, density stratification, and velocity profile are considered as controlling factors of the stability (all defined for near boundary layers), which means the R_i number is the ratio of perturbation force to inertia. The velocity profiles of several representative cross faces are plotted in Fig. 3(c) along the x direction. It is seen that the velocity shear is very steep near the boundaries. Such steep velocity gradients ensure that the boundary layer "tears" very easily. Then together with the thermal perturbation from the y direction, the main flow instability grows quickly with both time and space (Fig. 2; also see Ref. [19]).

The modified Richardson number is calculated for a several groups of inlet and boundary conditions. The calculated R_i shows some transition thresholds in stability diagram. As discussed in Ref. [19] the original KH instability can be formed by density gradient and/or velocity shear; the current microchannel KH instability happens in a similar way, only the instability source is density waves (or acoustic or perturbation waves) instead of gravity waves. It is found that below the R_i stability threshold, the near-critical flow is stable, with serrated boundary intrusions, and above the threshold vortex flow can be seen. For example, the critical values fall around

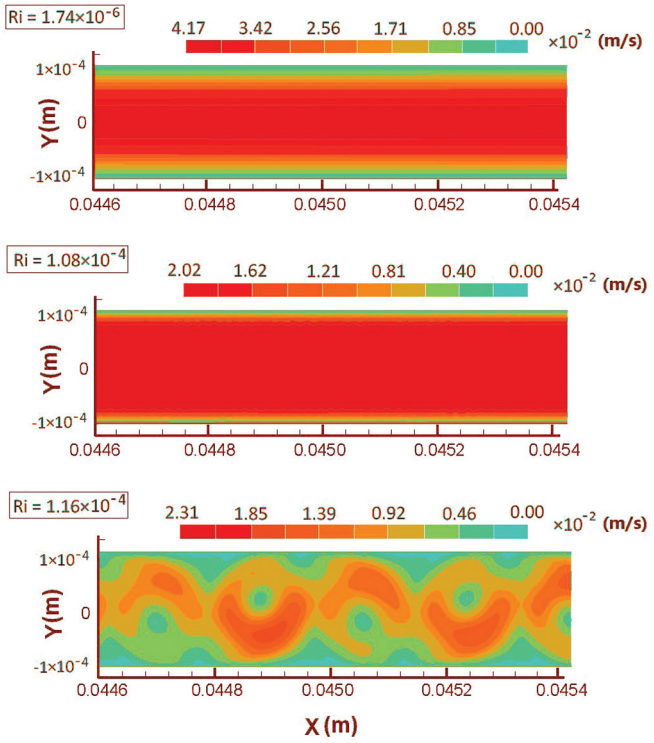

FIG. 4. (Color online) Respective velocity profile for each stability situation classified as stable flow, static serrated boundary invasion condition, and vortex flow in microchannels for $D = 2.0 \times 10^{-4}$ m, inlet Re = 26.80, captured for $t = 0.1$ s. By analogy to classical development of KH instability under gravity, a Richardson number R_i is defined as a function of boundary gradient of density, pressure, and velocity (perpendicular to the streamwise direction). For each channel size, channel expanding flow will go through some transitions from static laminar flow to vortex and unstable flow.

$R_i = 1.5 \times 10^{-5}$ for $D = 1.0 \times 10^{-4}$ m and $R_i = 1.1 \times 10^{-4}$ for $D = 2.0 \times 10^{-4}$ m, respectively, due to the effects of microchannel height conditions and respective spatial effects on viscous and density stratification processes. For the transition region of $D = 2.0 \times 10^{-4}$ m stable flow with serrated boundary intrusion is seen. The detailed convection structure can be seen in Fig. 4. Here it should also be noted that comparing with larger channel sizes, where the gravity effect cannot be neglected, the problem tends to be similar to the well-known Rayleigh-Bernard (RB) configuration, where HBL collapse will be dependent on the combination of heat perturbation and gravity induced buoyancy forces [9,16,20].

In addition, the current study also considered other inlet and initial conditions over a wide range. With the same physical origin, the microchannel flow will exhibit a similar transient instability evolution process. Also as discussed by Carles [21], high expandability and low thermal diffusivity are still significant even up to $\varepsilon_T = 0.3$, which indicates such phenomena will not disappear in a short distance from the critical point and may have application in a wide operational range. However, the current problem without gravity is not just one simple extension of the RB kind with instability only due to the stratification process (which follows, controlled by the Rayleigh criterion or Schwarzschild criterion), and respectively, the modified R_i where the pressure gradient and density gradient in the boundary serves as the main perturbation source as added to that Kelvin-Helmholtz stability evolution [19].

In summary, we studied the near-critical microchannel flow response to sudden heat input, with no gravity effect, and the transient equilibrium process was identified as a new Kelvin-Helmholtz instability. While in closed systems the PE is dominant, in open systems (microchannels) the thermal-mechanical expansion characteristics will lead to new instabilities, and a potential new area of microengineering under gravity or microgravity can be expected.

ACKNOWLEDGMENTS

This work is supported by Tohoku University (Japan) Global COE Program "World Center of Education and Research for Trans-Disciplinary Flow Dynamics" and also the Natural Science Foundation of China (Grant No. 50976002). The authors are very grateful to Professor B. Zappoli (Centre National D'Etudes Spatiales, France) and Professor D. Wood (University of Calgary, Canada) for useful communications and suggestions.

[1] B. Zappoli, C. R. Mec. **331**, 713 (2003).
[2] A. Onuki, H. Hao, and R. A. Ferrell, Phys. Rev. A **41**, 2256 (1990); H. Boukari, J. N. Shaumeyer, M. E. Briggs, and R. W. Gammon, *ibid.* **41**, 2260 (1990); B. Zappoli, D. Bailly, Y. Garrabos, B. Le Neindre, P. Guenoun, and D. Beysens, *ibid.* **41**, 2264 (1990).
[3] B. Zappoli, Phys. Fluids A **4**, 1040 (1992); T. Frohlich, D. Beysens, and Y. Garrabos, Phys. Rev. E **74**, 046307 (2006).
[4] D. Bailly and B. Zappoli, Phys. Rev. E **62**, 2353 (2000).
[5] A. Jounet, B. Zappoli, and A. Mojtabi, Phys. Rev. Lett. **84**, 3224 (2000).
[6] R. P. Behringer, A. Onuki, and H. Meyer, J. Low Temp. Phys. **81**, 71 (1990); H. Boukari, M. E. Briggs, J. N. Shaumeyer, and R. W. Gammon, Phys. Rev. Lett. **65**, 2654 (1990); F. Zhong and H. Meyer, Phys. Rev. E **51**, 3223 (1995).
[7] D. Beysens, D. Chatain, V. S. Nikolayev, J. Ouazzani, and Y. Garrabos, Phys. Rev. E **82**, 061126 (2010).
[8] M. Assenheimer and V. Steinberg, Phys. Rev. Lett. **70**, 3888 (1993); A. B. Kogan and H. Meyer, Phys. Rev. E **63**, 056310 (2001).
[9] S. Amiroudine and B. Zappoli, Phys. Rev. Lett. **90**, 105303 (2003).
[10] B. Zappoli and P. Carles, Eur. J. Mech. B/Fluids **14**, 41 (1995).
[11] B. Zappoli (private communication).
[12] B. Zappoli, S. Amiroudine, P. Carles, and J. Ouazzani, J. Fluid Mech. **316**, 53 (1996); S. Amiroudine, P. Bontoux, P. Larroud, B. Gilly, and B. Zappoli, *ibid.* **442**, 119 (2001).
[13] J. Straub, L. Eicher, and A. Haupt, Phys. Rev. E **51**, 5556 (1995); Y. Chiwata and A. Onuki, Phys. Rev. Lett. **87**, 144301 (2001).
[14] A. Jounet, A. Mojtabi, J. Ouazzani, and B. Zappoli, Phys. Fluids **12**, 197 (2000).

[15] NIST Standard Reference Database-REFPROP, Version 8.0, 2006.
[16] G. Accary, I. Raspo, P. Bontoux, and B. Zappoli, Phys. Fluids **17**, 104105 (2005).
[17] P. Carles, Phys. Fluids **18**, 126102 (2006).
[18] Pierre Carles and Kokou Dadzie, Phys. Rev. E **71**, 066310 (2005).
[19] Lord Kelvin (William Thomson), Philos. Mag. **42**, 362 (1871); S. Chandrasekhar, *Hydrodynamic and Hydromagnetic Stability* (Clarendon Press, Oxford, 1961).
[20] G. Accary, I. Raspo, P. Bontoux, and B. Zappoli, Adv. Space Res. **36**, 11 (2005); G. Accary, P. Bontoux, and B. Zappoli, Phys. Fluids **19**, 014104 (2007).
[21] P. Carles, J. Supercrit. Fluids **53**, 2 (2010).